

1 **Supplementary Materials**

2 **1 Materials and methods**

3 ***1.1 MTT assay***

4 Typically, exponentially growing MCF-7 and L929 cells were seeded in 96-well plates at 1×10^4
5 cells/well and pre-incubated for 24 hours. Then, the cells were incubated with Rg5, Rg5-BSA
6 NPs and FA-Rg5-BSA NPs at the Rg5-equivalent doses of 6.25, 12.5, 25, 50, and 100 μM for 24
7 and 48 hours. Subsequently, 50 μL of 0.5% MTT was added to each well and the cells were
8 incubated for 4 hours at 37 °C. Next, the medium was replaced with 150 μL of DMSO. The
9 optical density of the wells was measured at 490 nm using a microplate reader (Power Wave
10 XS2, BioTek Instruments Inc., USA).

11 ***1.2 Staining assay***

12 Briefly, the MCF-7 cells were cultured overnight in 6-well plates at a density of 2×10^5 cells/well in
13 2 mL medium. Then, Rg5, Rg5-BSA NPs and FA-Rg5-BSA NPs at 50 μM were added to the cells
14 separately for 24 hours. Cells treated with culture medium served as control. After the
15 supernatant was discarded and the cells were rinsed twice with PBS, the cells were stained with
16 Hoechst 33342 solution at 10 $\mu\text{g}/\text{mL}$ for 15 minutes in the dark, or with AO/EB staining solution at
17 2 $\mu\text{g}/\text{mL}$ for 5 minutes, then washed twice again with ice cold PBS. The stained cells were
18 observed using an inverted fluorescence microscope (Nikon, Tokyo, Japan).

19 **1.3 Confocal laser scanning microscopy**

20 The MCF-7 cells were seeded at a density of 4×10^4 cells/dish into a glass-bottom cell culture dish
21 (NEST, $\varnothing 90$ mm \times 20 mm, China) supplemented with folic acid-free medium or medium
22 containing 20 mM FA. Then, the medium was replaced with fresh medium containing
23 FITC-labeled Rg5-BSA NPs, FA-Rg5-BSA NPs, and FA-Rg5-BSA NPs plus 20 mM free FA (note:
24 the cells were pretreated with FA for one hour before adding FA-Rg5-BSA NPs to investigate if
25 FA specifically mediated cellular uptake) at the same concentration of 250 μ g/mL for 3 hours at
26 37 °C, respectively. After that, the culture medium was aspirated, and the cells were fixed and
27 stained with DAPI at 1 μ g/mL. Then, the cells were washed and imaged by confocal laser
28 scanning microscopy (CLSM, Olympus Fluoview FV-1000, Tokyo, Japan).

29 **1.4 Flow cytometry**

30 Typically, the MCF-7 cells were cultured in 6-well plates, grown overnight and then incubated
31 with free FITC, FITC-labeled Rg5-BSA NPs, FA-Rg5-BSA NPs, and FA-Rg5-BSA NPs plus 20
32 mM free FA with an equivalent FITC concentration of 250 μ g/mL for 3 hours at 37 °C. The
33 untreated cells served as control. After incubation, the suspension was removed and the wells
34 were washed with PBS to remove the NPs outside the cells. Subsequently, the samples were
35 trypsinized and harvested to obtain a cell suspension, and then resuspended in 200 μ L PBS for
36 flow cytometry analysis.

37 **1.5 Human breast cancer xenograft mouse model**

38 Five-week-old female BALB/c nude mice (16 ± 2 g) were purchased from Hunan SJA Lab Animal

39 Co., Ltd. (Hunan, China). They were humanely cared for with free water and food. Procedures
40 involving animals and their care were conducted in accordance with the National Institutes of
41 Health (NIH) guidelines and all animal experiments were performed in compliance with the
42 Animal Ethics Procedures and Guidelines of the People's Republic of China and approved by the
43 Northwest University Animal Ethics Committee.

44 To examine the in vivo anti-tumor effects of Rg5, Rg5-BSA NPs, and FA-Rg5-BSA NPs,
45 subcutaneous tumor xenograft models were established in the right limb armpit regions of nude
46 mice by injecting 1×10^7 MCF-7 cells/mouse/100 μ L after one week of acclimation. When the
47 tumors reached a volume of approximately 200 mm³, these mice were randomly divided into four
48 groups (n=6) (day 0), and injected intraperitoneally (i.p.) with the control, free Rg5, Rg5-BSA NPs,
49 and FA-Rg5-BSA NPs (15 mg/kg Rg5 equivalents) every day for three consecutive weeks.
50 During the treatment, the tumor volume was measured using a digital caliper, and the body
51 weights were monitored every 3 days. The tumor volume was calculated using the formula:
52 tumor volume (mm³) = (length) \times (width)² \times 0.5. After 21 days of treatment, the mice were
53 humanely sacrificed by cervical dislocation, dissected to obtain the tumors, then weighed and
54 imaged.

55 **2 Results and discussion**

56 ***2.1 The stability analysis***

57 The stability of nanoparticles in plasma determines the successful delivery of drug as it
58 prevents particle aggregation or embolism from occurring in the systemic circulation. As shown

59 in Figure S1, the Rg5-loaded nanoparticles in FBS were completely stable at 4 °C, as no
60 significant changes were observed in the particle size of Rg5-BSA NPs and FA-Rg5-BSA NPs
61 for 5 days. Because the negative zeta potential of the nanoparticles interacts with the negatively
62 charged components of the FBS to create a mutually exclusive force, the stability of
63 nanoparticles is maintained in FBS. Thus, this suggested that Rg5-loaded nanoparticles are
64 kinetically stable and propitious for further use as a drug carrier.

65 **2.2 TG analysis**

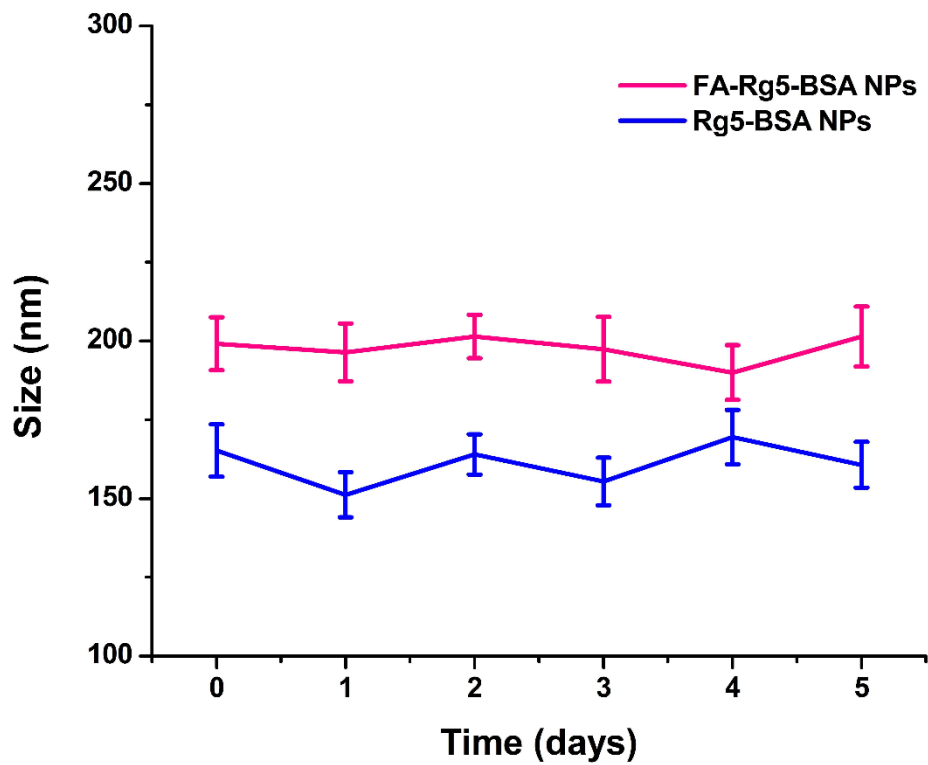
66 The thermal properties of BSA, Rg5, Rg5-BSA NPs, and FA-Rg5-BSA NPs were analyzed by TG
67 analysis. The TG data showed the stability of the nanoparticles and the degradation of the
68 materials with respect to increasing temperature. Figure S1 clearly showed that the Rg5-BSA
69 NPs began to lose weight at 100 °C, which was due to water loss, and started to degrade at
70 200 °C. A sudden drop in weight was found beyond 250 °C, due to the loss of small molecules,
71 ammonia and CO₂. As a result of FA, the FA-Rg5-BSA NPs underwent an abrupt decrease in
72 weight loss at the beginning. There were great differences in weight loss approximately 300 °C
73 for FA-Rg5-BSA NPs (28.94%), Rg5-BSA NPs (23.42%), Rg5 (10.91%), and BSA (24.95%).
74 Beyond 500 °C, a fast degradation ratio for Rg5-BSA NPs was observed compared to that for
75 BSA, which is attributed to the crystalline nature of Rg5 entrapped in Rg5-BSA NPs. However, a
76 relatively slower rate of degradation was observed in FA-Rg5-BSA NPs in the presence of FA. In
77 addition, beyond 600 °C, no obvious change was observed in BSA and Rg5-BSA NPs due to
78 char formation in the nitrogen atmosphere. The total reduction rate of weight loss was
79 approximately 41.14% for FA-Rg5-BSA NPs, 79.16% for Rg5-BSA NPs and 82.54% for Rg5. The

80 slow degradation rate of FA-Rg5-BSA NPs compared to that of Rg5, indicated the stability of the
81 FA-Rg5-BSA NPs.

82 **2.3 DSC analysis**

83 DSC thermograms could provide thermal behavior information, including new peaks,
84 endothermic peaks, peak shape, peak temperature, and enthalpy changes. DSC was utilized to
85 confirm the existing form of the Rg5 in the formulations and to investigate the interaction
86 between Rg5 and nanoparticles. A drug has better dissolution, absorption and bioavailability
87 when the drug within nanoparticles is in an amorphous state. Figure S2 showed the DSC
88 thermograms of BSA, Rg5, Rg5-BSA NPs, and FA-Rg5-BSA NPs. The Rg5 powders exhibited
89 an endothermic melting peak at 369.84 °C, which implied the crystalline nature of Rg5. However,
90 the characteristic peak of Rg5 disappeared in the thermogram of Rg5-BSA NPs and
91 FA-Rg5-BSA NPs, indicating that Rg5 was in an amorphous state after encapsulation into the
92 nanoparticles. While the DSC thermogram of FA-Rg5-BSA NPs showed a single peak at
93 137.38 °C, there was no peak near the Rg5-BSA NPs melting point, which confirmed the
94 formation of a nanodrug delivery system. This result indicated the stability of the obtained
95 product.

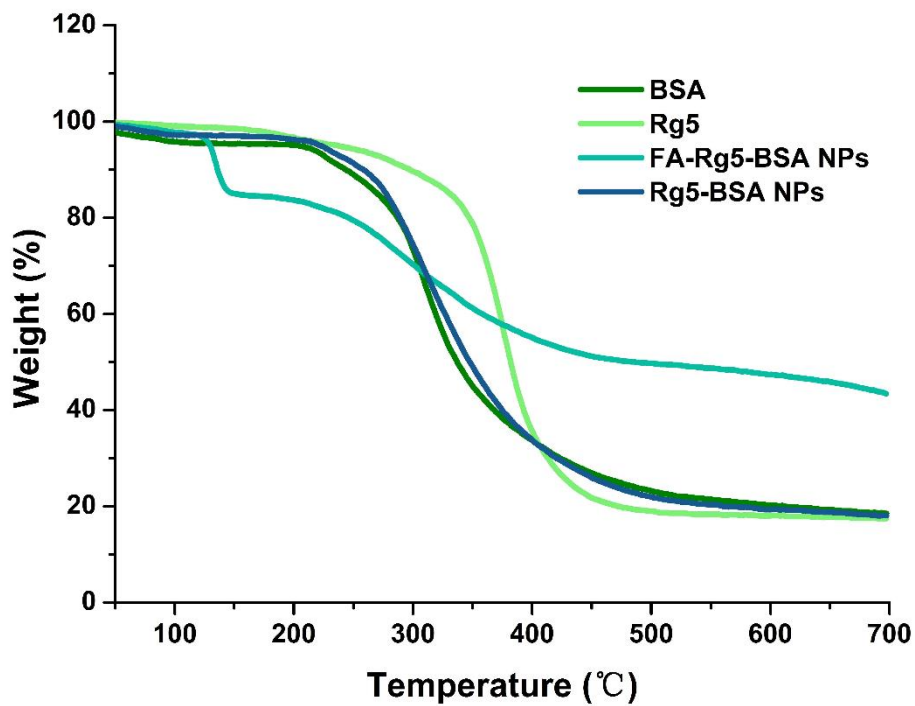
96



97

98 **Figure S1** The stability of Rg5-BSA NPs and FA-Rg5-BSA NPs in FBS. Data are represented as
99 mean \pm SD, n = 3.

100 **Abbreviations:** BSA, bovine serum albumin; Rg5, ginsenoside Rg5; FA, folic acid; NPs,
101 nanoparticles.

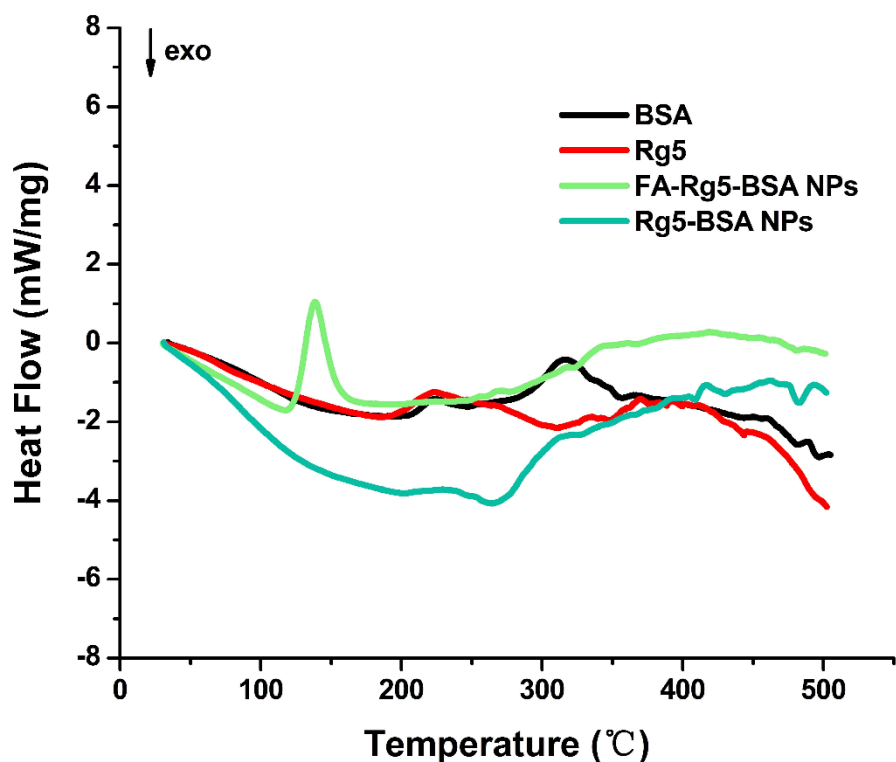


102

103 **Figure S2** TG analysis curves of BSA, Rg5, FA-Rg5-BSA NPs and Rg5-BSA NPs.

104 **Abbreviations:** BSA, bovine serum albumin; Rg5, ginsenoside Rg5; FA, folic acid; NPs,

105 nanoparticles; TG, thermo gravimetric.



106

107 **Figure S3** DSC analysis curves of BSA, Rg5, FA-Rg5-BSA NPs and Rg5-BSA NPs.

108 **Abbreviations:** BSA, bovine serum albumin; Rg5, ginsenoside Rg5; FA, folic acid; NPs,

109 nanoparticles; DSC, differential scanning calorimetry.

110

111 **Table S1** The effect of aqueous solution concentration of BSA on Rg5-BSA NPs

BSA concentration (mg/mL)	Particle size (nm)	PDI	Entrapment efficiency (%)
5	262.5±5.1	0.235±0.124	56.38±4.96
10	258.8±4.7	0.158±0.145	71.22±4.64
15	201.0±5.7	0.109±0.094	66.36±5.58
20	233.0±3.9	0.172±0.155	62.33±4.32

112

113 **Table S2** The effect of pH value of BSA solution on Rg5-BSA NPs

pH	Particle size (nm)	PDI	Entrapment efficiency (%)
7	301.4±6.1	0.154±0.143	53.21±3.77
8	277.6±5.6	0.097±0.069	69.37±5.19
9	223.5±4.4	0.119±0.106	75.36±4.44
10	321.4±5.3	0.236±0.213	81.56±5.67

114

115 **Table S3** The effect of volume ratio of ethanol to water on Rg5-BSA NPs

Volume ratio of ethanol to water	Particle size (nm)	PDI	Entrapment efficiency (%)
1	229.6±3.4	0.235±0.133	68.86±4.74
2	203.8±4.9	0.147±0.126	73.81±4.98
3	158.7±5.6	0.088±0.074	79.28±3.36
4	154.4±2.4	0.097±0.082	54.44±3.76

116

117 **Table S4** The effect of molar ratio of Rg5 to BSA on Rg5-BSA NPs

Molar ratio of Rg5 to BSA	Particle size (nm)	PDI	Entrapment efficiency (%)
5	243.8±3.5	0.115±0.084	59.28±2.95
10	233.6±5.2	0.212±0.146	66.44±3.88
15	199.7±4.1	0.083±0.062	69.54±2.79
20	174.8±3.0	0.072±0.053	87.29±2.55
25	209.6±4.7	0.229±0.185	77.63±3.50

118

119 **Table S5** The effect of the rate of adding ethanol on Rg5-BSA NPs

The rate of adding ethanol (mL/min)	Particle size (nm)	PDI	Entrapment efficiency (%)
0.1-1.0	229.6±3.4	0.117±0.096	60.35±2.95
1.0-1.5	203.8±4.9	0.214±0.185	77.38±3.28
1.5-2.0	160.7±3.1	0.073±0.064	75.43±2.84

120

121

Table S6 The effect of stirring speed on Rg5-BSA NPs

Stirring speed (r/min)	Particle size (nm)	PDI	Entrapment efficiency (%)
300	234.7±5.8	0.198±0.164	78.48±3.48
600	194.8±3.6	0.186±0.155	83.47±4.29
900	215.9±4.2	0.093±0.085	80.63±3.34

122

123

Table S7 The effect of stirring time on Rg5-BSA NPs

Stirring time (h)	Particle size (nm)	PDI	Entrapment efficiency (%)
6	255.7±5.3	0.081±0.066	59.29±4.17
12	208.3±2.6	0.131±0.104	63.28±3.74
24	198.6±3.3	0.076±0.062	75.65±4.11

124

125

Table S8 The effect of the molar ratio of folic acid to BSA on FA-Rg5-BSA NPs

Molar ratio of FA to BSA	Particle size (nm)	PDI	The amount of FA (µg/mg BSA NPs)
5	312.1±3.6	0.293±0.056	73.2±18.55
10	307.6±3.7	0.219±0.089	67.5±16.36

15	233.6±4.2	0.153±0.045	71.4±19.48
20	240.8±2.9	0.185±0.048	78.85±24.52

126

127 **Table S9** The effect of reaction time after adding folic acid on FA-Rg5-BSA NPs

Reaction time after adding FA (h)	Particle size (nm)	PDI	The amount of FA (µg/mg BSA NPs)
1	307.4±3.9	0.156±0.052	50.5±13.57
3	288.6±3.7	0.257±0.064	54.3±19.65
6	246.8±2.5	0.268±0.057	60.5±23.44
12	322.9±5.4	0.215±0.086	65.7±29.53

128

129 **Table S10** The effect of centrifugal speed on FA-Rg5-BSA NPs

Centrifugal speed (r/min)	Particle size (nm)	PDI	The amount of FA (µg/mg BSA NPs)
7000	267.4±3.5	0.179±0.096	63.42±23.83
10000	230.7±4.7	0.181±0.058	88.74±19.38
12000	209.5±4.6	0.278±0.045	53.79±27.46

130 **Notes:** Data are represented as mean ± SD, n = 3.

131 **Abbreviations:** BSA, bovine serum albumin; Rg5, ginsenoside Rg5; FA, folic acid; NPs,

132 nanoparticles.